Deuteron Stripping Reaction on Mg^{25}†

R. B. WEINBERG, G. E. MITCHELL, AND L. J. LIDOFSKY
Columbia University, New York, New York
(Received 25 September 1963)

The $Mg^{25}(d,p)Mg^{26}$ reaction was studied at bombarding energies between 3.0 and 5.2 MeV. Angular distributions were measured for proton groups to the ground state and four excited states of Mg^{26}. The elastic scattering in the entrance and exit channels was measured at the appropriate energies and optical-model parameters determined. Using the distorted-wave Born approximation, spectroscopic factors were extracted from the stripping data. Except for the ground state (pure $l=2$), a mixture of l values ($l=0$ and 2) was required to fit the data.

I. INTRODUCTION

THE collective model has provided a rather satisfactory description of the properties of the low-lying levels of odd-A nuclei in the $2s$-$1d$ shell. For the even-mass nuclei in this region, the theoretical situation is more complex. One promising nucleus for study is Mg^{26}, since it is created by adding one neutron to Mg^{25}, for which the collective model description is satisfactory. A reaction which is appropriate for the study of the low-lying levels in Mg^{26} is $Mg^{25}(d,p)Mg^{26}$. The (d,p) reaction corresponds to a single nucleon transfer that couples the states of interest directly to the ground state of Mg^{25}. From the point of view of theory, the reaction mechanism is reasonably well understood. Experimentally this reaction is convenient; it is highly exoergic, the low-lying levels in Mg^{26} are well separated, the targets are relatively easy to fabricate, and the isotope is available in high enrichments.

In the present experiment,[1] a large number of angular distributions were measured. The data were analyzed using the distorted-wave Born approximation (DWBA). In this treatment, stripping is considered as a perturbation to elastic scattering. To reduce the number of free parameters in the DWBA calculation, the elastic scattering of deuterons from Mg^{25} and of protons from Mg^{26} was measured. The optical model parameters were determined by fitting these elastic-scattering angular distributions. Using the DWBA, relative reduced widths for the various levels in Mg^{26} were determined. By extracting reduced widths at a variety of energies, one can minimize the ambiguities resulting from compound nuclear contributions. Information about the structure of Mg^{26} can be inferred from these widths.

The experimental apparatus and procedure is described in Sec. II. A discussion of the data processing is given in the next section, with emphasis upon the utilization of high-speed digital computers. The elastic scattering data are presented in Sec. IV and the optical-model analysis discussed. Section V is devoted to the analysis of these data using the DWBA. The final section summarizes the results.

II. EXPERIMENTAL APPARATUS AND PROCEDURE

A. Targets

The magnesium isotopes were obtained from Oak Ridge National Laboratory in the form of magnesium oxide. Enrichments were 97–99% of the desired isotope. Targets were prepared by an evaporation procedure in which magnesium oxide was mixed with pure tantalum powder, placed in a tantalum "boat" and heated. The oxide was reduced by the tantalum, and the resulting, nearly pure, magnesium evaporated onto thin foils. The Mg^{25} targets were approximately 300 $\mu g/cm^2$ thick, on Formavar backings of less than 20 $\mu g/cm^2$ thick. The Mg^{26} targets were approximately 300 $\mu g/cm^2$ thick on 500-$\mu g/cm^2$ nickel backings.

B. Apparatus

The $Mg^{25}(d,d)Mg^{25}$ and the $Mg^{25}(d,p)Mg^{26}$ experiments were performed, using the Columbia University 5.5-MeV Van de Graaff accelerator as a source of charged particles. The large cylindrical (48-in. diam, 60-in. height) scattering chamber[2] was used for these experiments. The angular positions of the detectors were remotely controlled through a system utilizing "Slo-Syn" motors.[3]

The elastically scattered deuterons were observed with a surface-barrier solid-state detector. A charge-sensitive preamplifier was used, followed by standard detection electronics. The protons from the (d,p) reaction were observed with a thin (0.025-in.) NaI crystal mounted upon an RCA 6342A photomultiplier tube. The data were accumulated on an RCL 512 channel analyzer.

In the exit channel, the protons are at energies well beyond the range of our Van de Graaff accelerator (since the ground-state Q value is 8.87 MeV). Therefore, the

† Work partially supported by the U. S. Atomic Energy Commission.

[1] R. B. Weinberg, G. E. Mitchell, and L. J. Lidofsky, Bull. Am. Phys. Soc. 8, 127 (1963); G. E. Mitchell, R. B. Weinberg, and L. J. Lidofsky, *ibid.* 8, 318 (1963); R. B. Weinberg, G. E. Mitchell, R. Horoshko, P. E. Osmon, and L. J. Lidofsky, *ibid.* 8, 318 (1963).

[2] R. Weinberg, H. M. Dowds, and L. J. Lidofsky, Bull. Am. Phys. Soc. 6, 307 (1961).

[3] Superior Electric Company, Bristol, Connecticut, Model SS-50-P1.

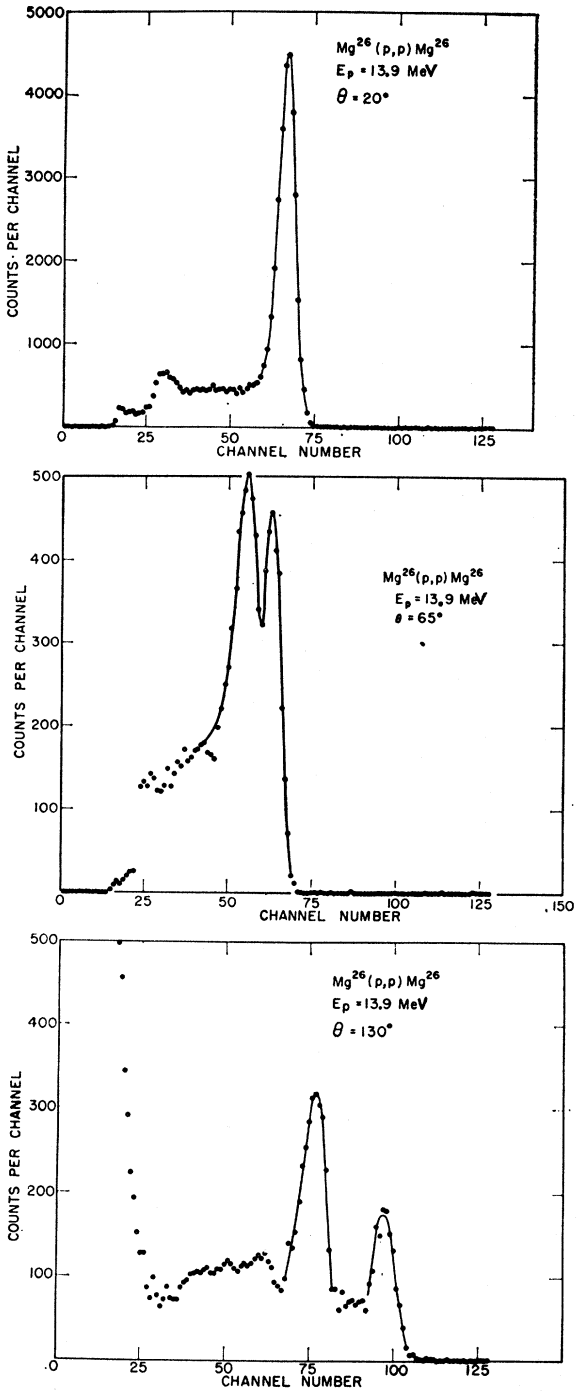

FIG. 1. Pulse-height distributions for protons elastically scattered from Mg^{26}.

external beam of the Columbia University 37-in. cyclotron was used as a source of 13.9-MeV protons. Aluminum absorbing foils were used to degrade the proton energy sufficiently, so that the protons were completely stopped in the solid state detector. To reduce nonuniformity in the absorbing foils, a large number of very thin foils (oriented in a random fashion) were used. The electronics were standard.

C. Procedure

1. $Mg^{26}(p,p)Mg^{26}$ *angular distribution.* In this experiment, the elastic proton groups from magnesium and from nickel could not be separated forward of about 70°. Some typical pulse-height distributions are shown in Fig. 1. At the forward angles, separate runs were made using a magnesium-plus-nickel target, and a nickel target. A normalization was determined at back angles, and the contribution due to nickel at forward angles was then subtracted. This procedure worked rather well in practice. An angular distribution was measured at $E_p = 13.9$ MeV. The assumption was made that the elastic scattering at 20° was completely due to Coulomb effects, and the absolute differential cross section evaluated on the basis of this assumption.

2. $Mg^{25}(d,d)Mg^{25}$ *angular-distribution and excitation functions.* In the deuteron elastic-scattering measurements, the elastic groups from magnesium, carbon, and oxygen could not be separated forward of about 45°. Separate runs were made using a magnesium-plus-Formvar target, and a Formvar target. After determining an appropriate normalization, a subtraction procedure was followed to extract the $Mg^{25}(d,d)Mg^{25}$ cross sections. In contrast to the proton elastic scattering experiment, this subtraction procedure was not completely successful. The difficulties are attributed to the different relative amounts of oxygen and carbon in the two targets and to the presence of high-energy proton groups from the $Mg^{25}(d,p)Mg^{26}$ reaction which were not completely stopped in the detector. As a result, forward-angle data were extracted for the deuteron elastic

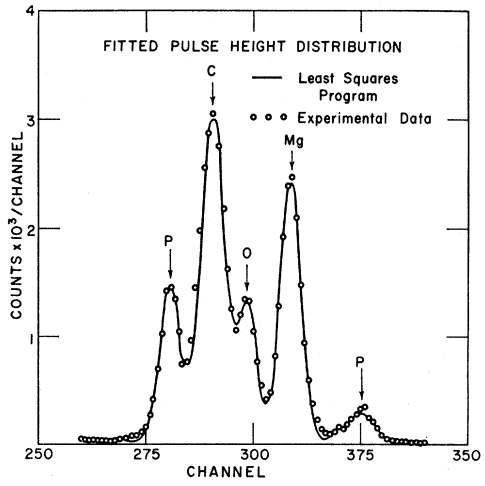

FIG. 2. Pulse-height distribution for elastically scattered deuterons. The peaks marked Mg, O, and C are due to elastic scattering of deuterons from these elements; the peaks marked *p* are due to protons which have passed completely through the detector. The solid curve is the result of calculations using the least-squares program described in the text.

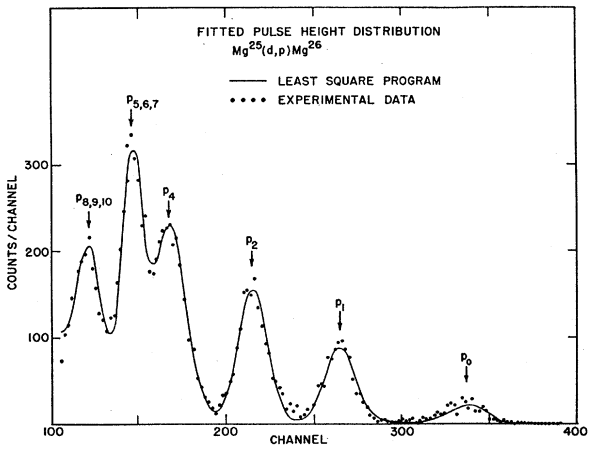

FIG. 3. A typical pulse-height distribution for protons from the $Mg^{25}(d,p)Mg^{26}$ reaction. The solid curve is the result of the least-squares fit.

scattering at only the two lowest energies. However, the elastic-scattering angular distributions appear to depart rather slowly and uniformly from Rutherford scattering. All of the optical-model calculations also show this behavior even at the highest energies involved in this experiment. Therefore, the lack of these data does not appear very important. Eight angular distributions were measured throughout the deuteron energy range from 3.0 to 5.2 MeV. In addition, excitation functions were determined at 60° and 130° from 3.0 to 5.5 MeV. The data were normalized to Rutherford scattering using the forward-angle data at 3.03 and 3.28 MeV.

3. $Mg(d,p)Mg^{26}$ *angular distributions and excitation functions.* There were no problems of interpretation with the (d,p) spectra, since the proton groups of interest were higher in energy than groups from any major contaminants. Ten angular distributions were measured throughout the energy range of 3.0 to 5.2 MeV. The cross sections for the (d,p) reaction were determined by observing the elastically scattered deuterons and two of the proton groups in the same geometry (with a solid-state detector), and normalizing the relative proton cross sections to the previously determined elastic cross sections. Excitation functions for the $(d,p_{0,1,2})$ reactions were determined at 20°, 60°, and 130°.

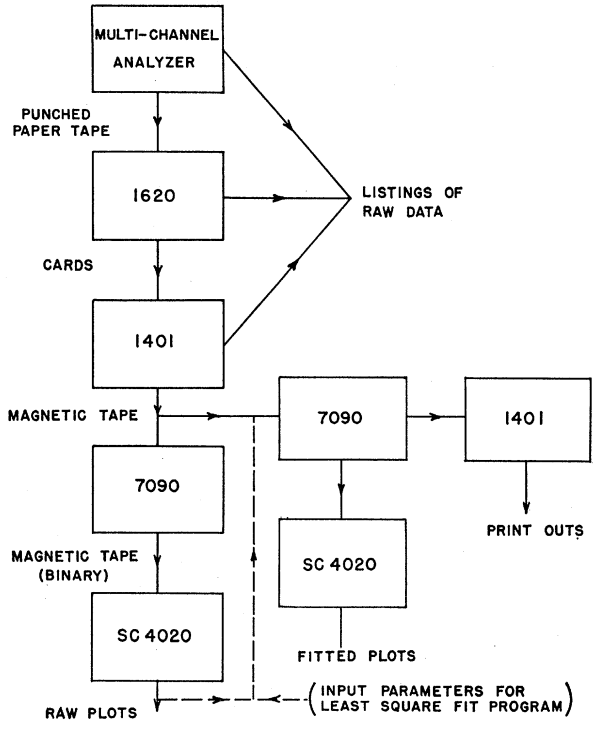

FIG. 4. Block diagram of the data processing procedure.

III. DATA PROCESSING

Typical pulse-height distributions for the (d,d) and (d,p) experiments are shown in Figs. 2 and 3. In order to process the data from 600 such spectra in a reasonable length of time, and in order to extract the maximum possible information, high-speed digital computers were utilized. In practice, the time required to set up a working data processing system was much less than would have been required to process even a small fraction of the data from this one experiment by desk calculator techniques.

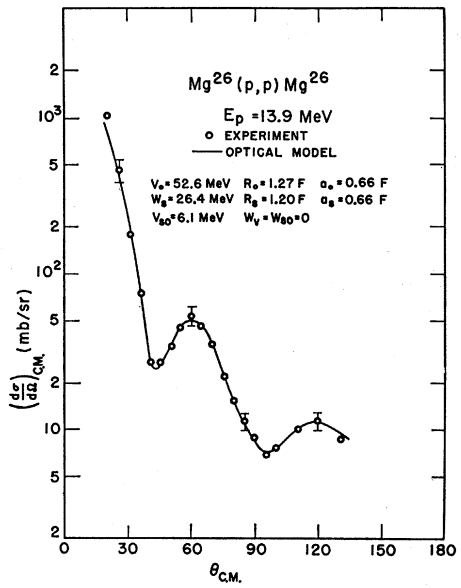

FIG. 5. Elastic scattering of protons from Mg^{26}. The solid curve is the result of an optical-model calculation using the parameters listed in the drawing.

The data processing procedure is shown diagrammatically in Fig. 4. The output from the multichannel analyzer is punched paper tape. The first stage in the process is to transfer the data to magnetic tape. The particular digital equipment available required that this

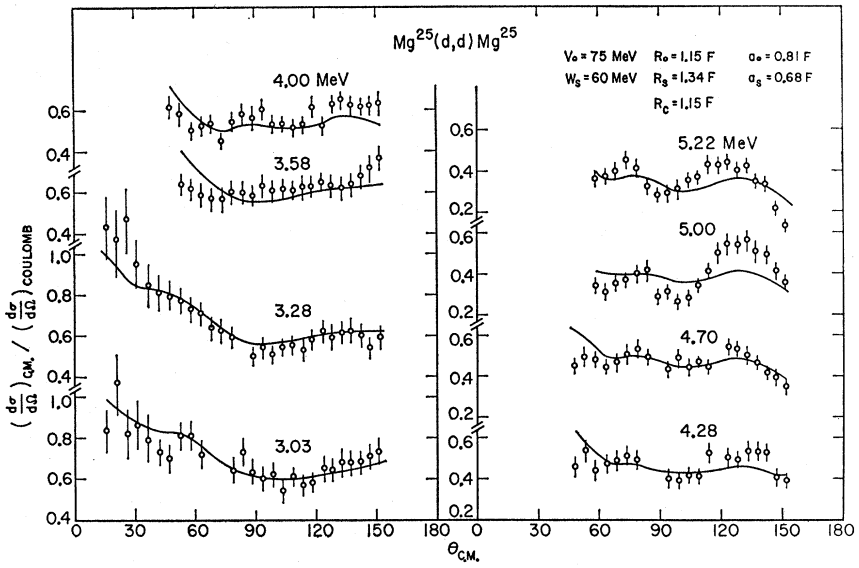

FIG. 6. Elastic scattering of deuterons from Mg^{25}. The solid curves are the results of optical-model calculations using the parameters listed in the drawing.

be done in two separate steps—punched paper tape to punched cards with an IBM-1620 computer, punched cards to magnetic tape with an IBM-1401 computer. Plots of the raw data were produced using a SC-4020 high-speed plotter.

The actual data analysis was performed with the aid of a least-squares-fit program developed at Los Alamos,[4] which uses an expression of the form

$$y=\sum_i A_i \exp-\left(\frac{x_i-x_{0i}}{\Delta x_i}\right)^2,$$

with A_i, x_{oi}, and Δx_i as the parameters to be varied. The first approximations supplied to this program (number of peaks, height, location, width for each) were obtained by visual inspection. A direct printed listing was obtained, which included final values of all parameters, the area under each peak, and a final point-by-point comparison of experimental and calculated values. A second output of the fitting program is a magnetic tape which serves as an input for the SC-4020. In the second set of plots obtained from the SC-4020, the calculated curve is superimposed upon the raw data. This provides a convenient visual check for evaluating the fit. Typical results are shown in Figs. 2 and 3.

IV. RESULTS AND ANALYSIS ELASTIC SCATTERING ANGULAR DISTRIBUTIONS

The differential cross section for $Mg^{26}(p,p)Mg^{26}$ is shown in Fig. 5. Each point has a 5% error due to statistics and uncertainty in background subtraction. The data between 20° and 50° have an additional error of about 15% due to the uncertainties in subtracting the contribution due to the nickel backing. The absolute cross-section scale is dependent upon the assumption that the scattering is purely Coulomb at 20°. The magnitude of the cross section and the shape of the angular distribution is not very different from that measured previously at 18 MeV.[5]

The data were fit using an optical potential of the form:

$$U=V_{\text{Coulomb}}+V+iW+V_{s0}+iW_{s0}$$

$$V=\frac{-V_0}{1+e^x},\quad x=\frac{r-r_0A^{\frac{1}{3}}}{a_0},$$

$$W=-\left(W_0+W_s\frac{d}{dx'}\right)\frac{1}{1+e^{x'}},\quad x'=\frac{r-r_sA^{\frac{1}{3}}}{a_s},$$

$$V_{s0}=-V_{s0}\left(\frac{h}{m_\pi c^2}\right)^2\left[\frac{1}{r}\frac{d}{dr}\left(\frac{1}{1+e^x}\right)\right]\mathbf{l}\cdot\mathbf{s}.$$

W_{s0} was set to 0 for the present work.

Initial estimates for the parameters of the optical potential were selected to be consistent with those previously used in this general mass and energy region. These estimates and the experimental data were then used in the Oak Ridge optical model search code "Hunter." The best fit is shown in Fig. 5.

For the deuteron elastic scattering, the angular distributions show relatively weak structure. This structure is accentuated in a plot of the experimental cross section divided by the Coulomb cross section. This is shown in Fig. 6. Each point has a 10% error arising from statistical and background-subtraction considerations. The forward-angle data at 3.03 and 3.28 MeV have a larger error due to the difficulties described earlier.

In the fitting of the deuteron data, the spin-orbit

[4] P. McWilliams, W. S. Hall, and H. E. Wegner, Rev. Sci. Instr. 33, 70 (1962).

[5] G. Schrank, E. K. Warburton, and W. W. Daehnick, Phys. Rev. 127, 2159 (1962).

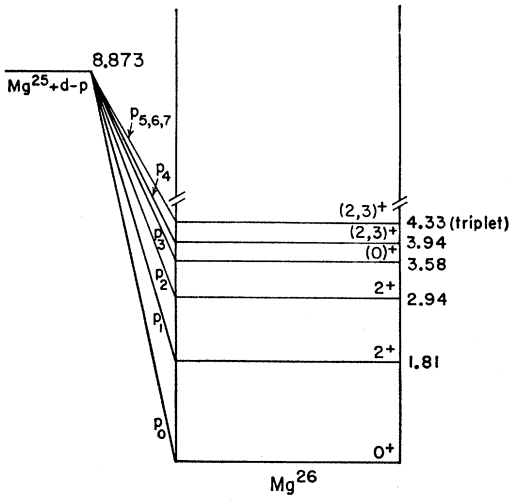

FIG. 7. Level scheme for the low-lying levels of Mg^{26}.

terms in the optical potential were ignored and searches were performed using the experimental data taken at 3.28 MeV. Without much difficulty, four sets of parameters were found which fit the data equally well—two with surface absorbtion, two with volume absorbtion. For volume absorbtion, the real potential is about 85 MeV, the imaginary potential about 20 MeV. Using the parameters determined from the search at 3.28 MeV (assuming surface absorbtion), angular distributions were calculated at various energies. These results are shown in Fig. 6. The parameters used are listed on the drawing. Improved fits could of course have been obtained if the parameters were varied from energy to energy. However, these four rather different sets of parameters, when entered in the DWBA calculations led to similar results for the (d,p) angular distributions. The particular set given in Fig. 6 was considered as physically most reasonable and so was selected for final calculations.

V. (d,p) RESULTS AND ANALYSIS

A. Results

The level scheme[6] for Mg^{26} is shown in Fig. 7. Angular distributions were measured at 10 energies between 3.0 and 5.2 MeV for protons to the ground and low-lying excited states of Mg^{26}. The p_3 group was not observed in this experiment. The ground state group was often rather weak and as a result, angular distributions could not be obtained at several energies. The measured angular distributions are shown in Figs. 8, 9, 10, 11, and 12. The relative error of about 5% on each data point is primarily statistical in nature. The excitation functions confirmed the energy-to-energy normalizations to about 10%.

Some qualitative comments can be made concerning the data. Except for the proton group to the first excited state, the angular distributions of all of the different groups show a rather regular behavior as function of energy. The variation in the angular distributions of (d,p_1) is confirmed by the presence of a broad anomaly in the excitation function at 20°. This is shown in Fig. 13. By contrast, the elastic scattering excitation curves are very smooth, as shown in Fig. 14. Therefore, the fluctuations are in the p_1 channel. The (d,p) angular distributions were compared with earlier measurements performed on this reaction at 2.99 MeV.[7] While the shape and absolute cross section for (d,p_2) was in excel-

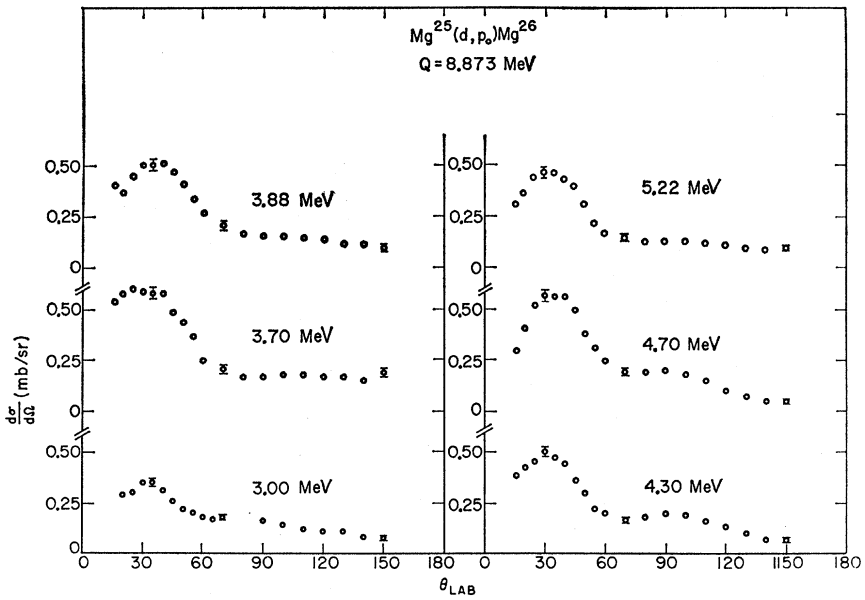

FIG. 8. Angular distributions for the $Mg^{25}(d,p_0)Mg^{26}$ reaction.

[6] P. M. Endt and C. Van der Leun, Nucl. Phys. **34**, 1 (1962).
[7] J. Takano, Phys. Soc. Japan **16**, 598 (1961).

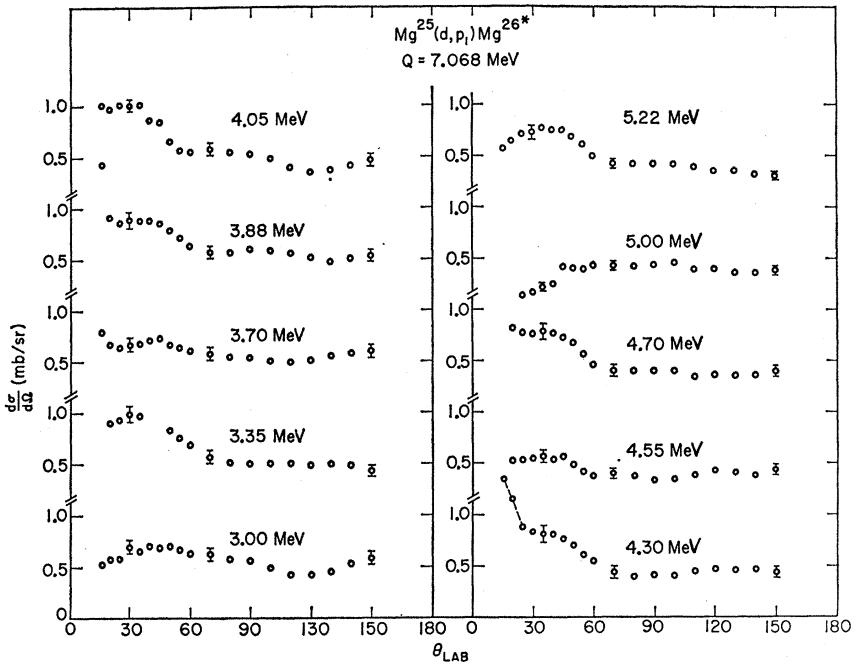

FIG. 9. Angular distributions for the $Mg^{25}(d,p_1)Mg^{26*}$ reaction. Note the fluctuations at forward angles, especially at the higher energies.

lent agreement, there was disagreement concerning the behavior of the (d,p_1) angular distribution at forward angles. Unexplained fluctuations at forward angles were also observed by Hamburger[8] in the $Mg^{24}(d,p_0)Mg^{25}$ reaction.

B. Analysis

The distorted-wave Born approximation has been described in detail.[9] Here only sufficient description is given to make the discussion clear. The differential cross sections for the stripping reaction can be conveniently written as

$$\frac{d\sigma}{d\Omega}=\frac{2J_f+1}{2J_i+1}\sum_{lsj} S_{lsj}\sigma_{lsj}(\theta).$$

The spectroscopic factor[10] is related to the usual reduced width by $S=\theta^2/\theta_0^2$, where θ^2 is the reduced width for the

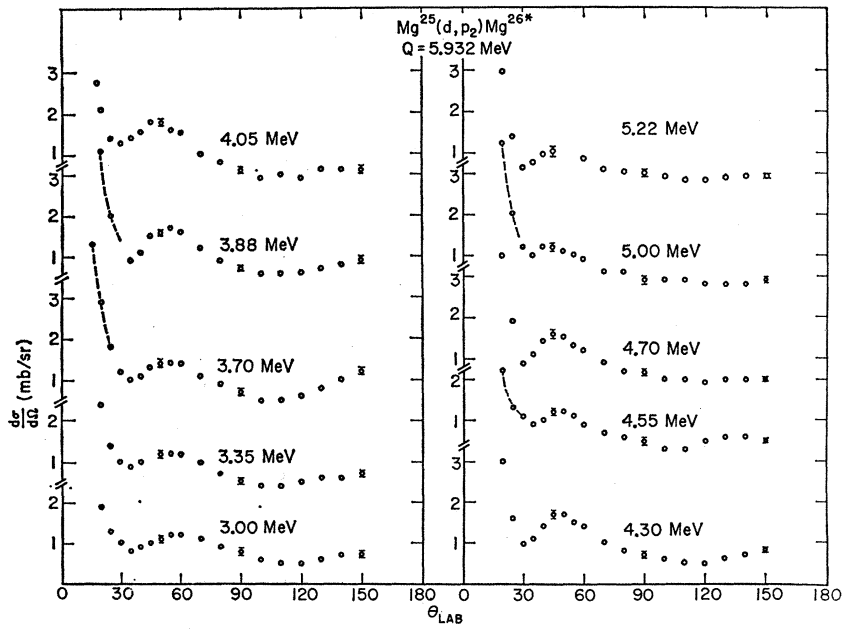

FIG. 10. Angular distributions for the $Mg^{25}(d,p_2)Mg^{26*}$ reaction.

[8] E. W. Hamburger and A. G. Blair, Phys. Rev. **119**, 777 (1960).
[9] R. H. Bassel, R. M. Drisko, and G. R. Satchler, Oak Ridge National Laboratory Report ORNL-3240, 1962 (unpublished); R. H. Bassel, G. R. Satchler, R. M. Drisko, and E. Rost, Phys. Rev. **128**, 2693 (1962); E. Rost, Phys. Rev. **128**, 2708 (1962).
[10] M. H. MacFarlane and J. B. French, Rev. Mod. Phys. **32**, 567 (1960).

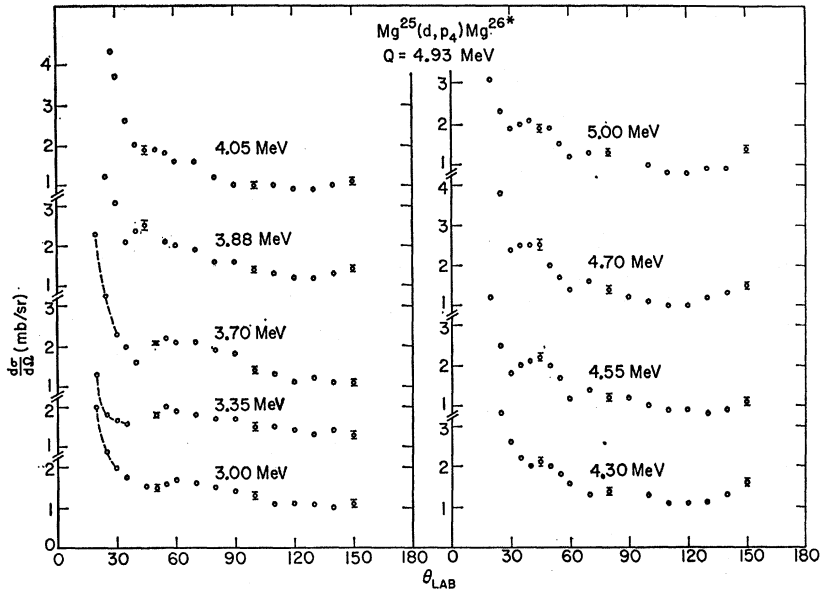

FIG. 11. Angular distributions for the $Mg^{25}(d,p_4)Mg^{26*}$ reaction.

transition and, θ_0^2 is the single particle reduced width. The single particle reduced width is defined in terms of the radial wave function of the transferred neutron—

$$\theta_0^2 = r_0 R_l^2(r_0)/3.$$

The cross section $\sigma_{lsj}(\theta)$ was calculated using the Oak Ridge DWBA code "Julie." A pure s-state wave function of the Hulthen form was assumed for the internal motion of the deuteron. The bound-state wave function for the captured neutron is a harmonic oscillator function (principal quantum number N, orbital angular momentum l, binding energy $B_N = Q + 2.23$), which was matched smoothly to a negative-energy Coulomb function at $r = R_N$.

The simplest case studied was the ground-state reaction, for which angular momentum and parity conservation require $l=2$. The angular distribution calculated using DWBA is shown in Fig. 10. For all of the other groups the restriction to a single l value does not apply, and in fact a number of different l values were required in order to fit the data. As an example of the procedure followed, consider the (d,p_2) angular distribution at 3.35 MeV. A neutron captured to form the second excited state of Mg^{26} may have $l=0$, 2, or 4; however, there is no evidence for any appreciable $l=4$ contribution. The angular distribution for $l=0$ capture showed a very sharp dip in the vicinity of 35° almost independent of the parameters used. Therefore, it was assumed that all of the cross section at 35° was due to $l=2$ capture. This determines the upper limit of the $l=2$ part

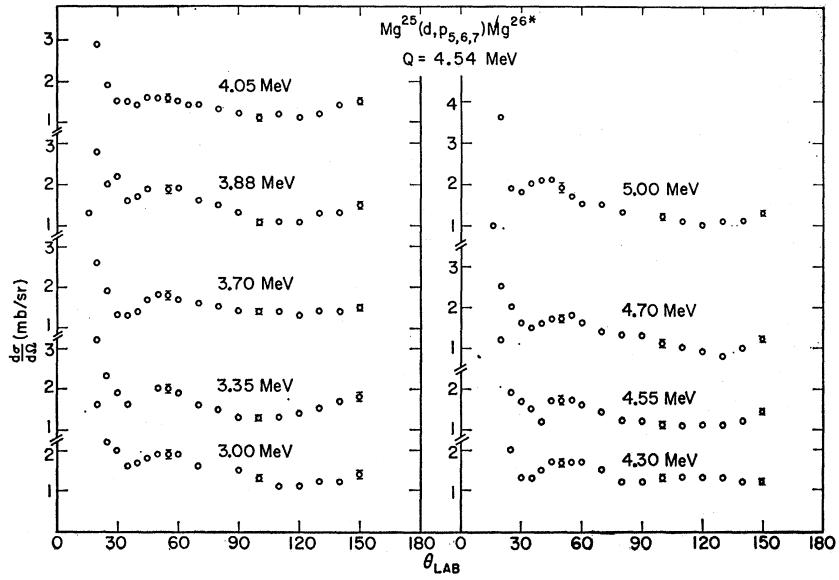

FIG. 12. Angular distributions for the $Mg^{25}(d,p_{5,6,7})Mg^{26*}$ reaction.

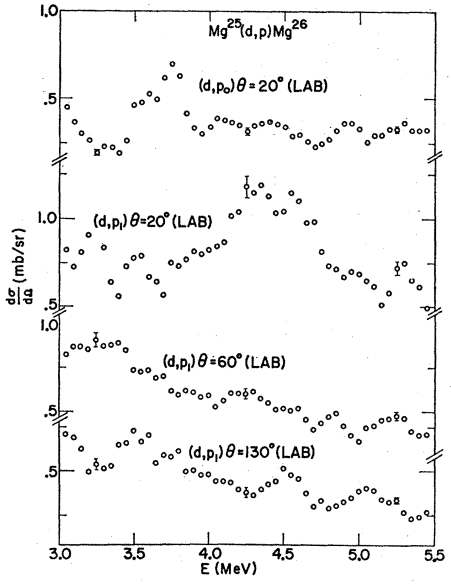

FIG. 13. Excitation functions for the $Mg^{25}(d,p)Mg^{26}$ reaction.

of the spectroscopic factor. The $l=2$ angular distribution calculated for this value of S was subtracted from the experimental data, and the remainder fit assuming $l=0$ neutron capture. Fits obtained with this sort of mixture are quite reasonable, as shown in Fig. 16.

The extracted spectroscopic factors are listed in Table I. The fluctuating cross section of the p_1 group at forward angles leads to a varying spectroscopic factor (for the $l=0$ part) and, therefore, the S value for the p_1 group is enclosed in parenthesis to denote the large uncertainty. The spins of the fourth excited state and the triplet around 4.33 MeV are not definitely known.

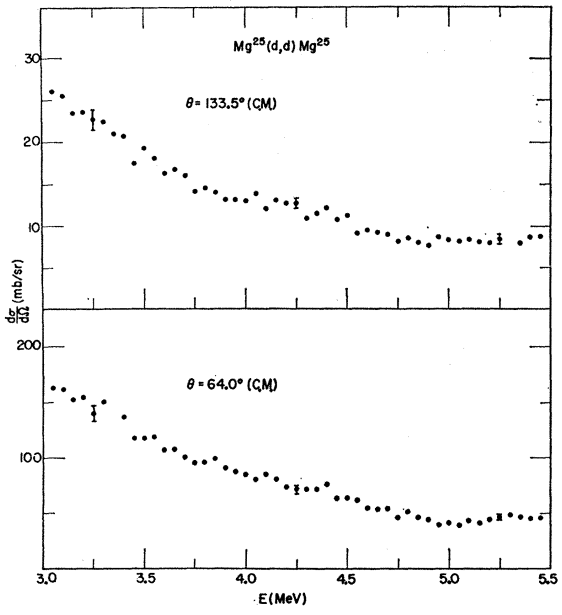

FIG. 14. Excitation functions for the $Mg^{25}(d,d)Mg^{25}$ reaction.

TABLE I. The spectroscopic values extracted from the DWBA fitting to the experimental data. The values quoted are averages. For the 1.81-MeV state, the $S_{l=0}$ factor fluctuates wildly as a function of energy.

E_{ex}	J^π	$S_{l=2}$	$S_{l=0}$	$(S_{l=2}/S_{l=2})_{\text{ground state}}$
0	0+	6.3	0	1
1.81	2+	0.5	(0.2)	0.09±0.04
2.94	2+	0.7	0.7	0.11±0.04
3.94	2, 3+	1.0, 0.8	1.0, 0.8	0.14±0.05
4.33	2, 3+	0.8, 0.6	0.8, 0.6	0.11±0.04

Spectroscopic factors corresponding to J_f equal to 2 and 3 are therefore included.

The shapes calculated with DWBA do not appear to be sensitive to small changes in the optical-model parameters. The magnitude of the DWBA cross section

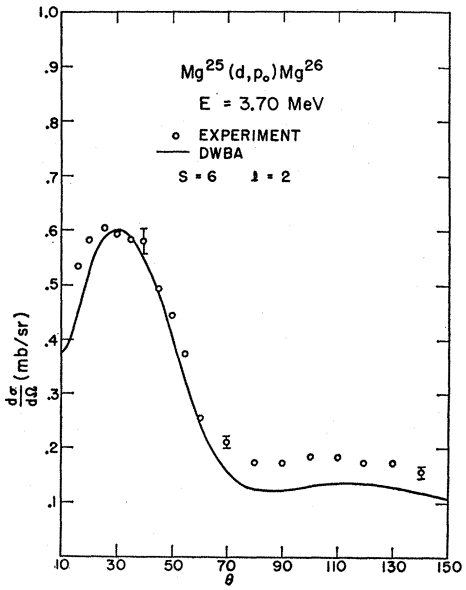

FIG. 15. DWBA fit to the (d,p_0) angular distribution at 3.70 MeV.

$[\sigma_{lsj}(\theta)]$ does change, and therefore the values of S change. However, ratios of spectroscopic factors (or ratios of cross sections) appear to be much less sensitive to variations of these parameters. The ratios $S_{l=2}$ (excited states)/$S_{l=2}$(ground state) listed in the table are averages.

The ratio $S_{l=2}$(first excited state)/$S_{l=2}$ (ground state) is of particular interest. The values of this ratio, at all energies at which angular distributions for both groups were measured, are listed in Table II. Assuming that the ground state and the first excited state of Mg^{26} are members of a rotational band, MacFarlane and French[10] calculated this ratio to be 0.36. The average value for the ratio determined from the DWBA fits to the data is about 0.09. The first excited state is clearly not a pure state in the ground-state band. The amount of mixing inferred here can only be considered qualitatively correct, due to the various uncertainties and

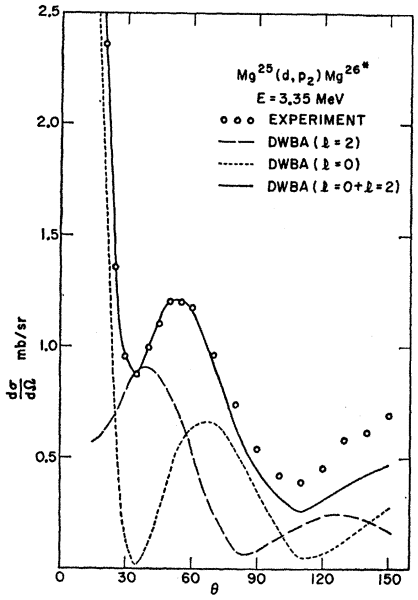

FIG. 16. DWBA fit to the (d,p_2) angular distribution at 3.35 MeV. The two dashed curves show the $l=0$ and $l=2$ contributions. The solid curve is the sum of these two contributions.

approximations involved in the calculation of the S_l's. However, the qualitative fits to the experimental data are quite satisfactory.

TABLE II. The energy dependence of $S_{l=2}$ factors for the ground and first excited state.

E_{lab}	$S_{l=2}$ (ground state)	$S_{l=2}$ (1st excited state)	(S 1st/ S ground)$_{l=2}$
3.05	7.0	0.64	0.09
3.70	8.5	0.60	0.07
3.88	6.9	0.59	0.09
4.30	5.2	0.50	0.10
4.70	6.2	0.50	0.08
5.22	4.2	0.31	0.07

VI. SUMMARY

The present work was undertaken primarily to obtain information about the low-lying levels in Mg^{26}. In order to obtain better values for the various reduced widths, angular distributions of the stripping reaction were measured at a variety of energies, and the elastic scattering in both the entrance and exit channels was also measured. Reasonable fits to the proton and deuteron elastic scattering were obtained using an optical model, although there is ambiguity in the choice of optical-model parameters for the deuteron elastic scattering. This ambiguity and most of the other uncertainties critically affect only the absolute values of the cross sections (and thus the spectroscopic factors) in the DWBA calculation. For this reason only ratios of spectroscopic factors are compared with theoretical predictions.

Satisfactory fits were obtained to almost all of the angular distributions. The cross section of the p_1 group shows an anomalous fluctuation with energy (at forward angles).

Except for the ground state, a mixture of l values ($l=0$ and 2) was required to fit all of the (d,p) data. The experimental value of the ratio $S_{l=2}$(first excited state)/$S_{l=2}$(ground state) is about 0.09, as compared with the value of 0.36 obtained by MacFarlane and French[10] assuming a pure rotational band.

ACKNOWLEDGMENTS

The authors wish to express their gratitude to Dr. R. Bassel and Dr. R. Drisko of Oak Ridge National Laboratory for their assistance in the performing of the theoretical calculations. Thanks are also due to Mr. J. Ostrowski for developing the technique for making the targets; to Dr. P. Osmon and Mr. R. Horoshko for their help in performing the experiment; and to Miss C. Browne for her work in the various phases of the computer operation.

The authors also wish to acknowledge their indebtedness to Dr. R. Jastrow and Dr. K. King and their respective staffs at the NASA and Columbia computing facilities.

The authors would especially like to thank Dr. B. Cujec for pointing out an error in an earlier version of this paper.